Heliyon 10 (2024) e35839

Contents lists available at ScienceDirect

Heliyon

journal homepage: www.cell.com/heliyon

Research article

Comprehensive analysis of malabar tamarind fruit rind total extract: HPTLC fingerprinting, *in-silico* exploration of its metabolites for SARS-cov-2 omicron spike protein, antibacterial and antidiabetic potentials with *in vitro* evaluation of antidiabetic and antioxidant activities

Hanan Khojah [a], Ehab M. Mostafa [b,c], Asail A. Aljounaidi [b], Abdulrahman M. Saleh [d,e], Mohammad El-Nablaway [f,g], Ahmed Ismail [h,*]

[a] Department of Pharmacy, College of Pharmacy, Nursing and Medical Sciences, Riyadh Elm University, Riyadh, Saudi Arabia
[b] Department of Pharmacognosy, College of Pharmacy, Jouf University, Sakaka, Saudi Arabia
[c] Pharmacognosy and Medicinal Plants Department, Faculty of Pharmacy (Boys), Al-Azhar University,Cairo, 11884, Egypt
[d] Pharmaceutical Medicinal Chemistry & Drug Design Department, Faculty of Pharmacy (Boys), Al-Azhar University, Cairo, 11884, Egypt
[e] Epidemiological Surveillance Unit, Aweash El-Hagar Family Medicine Center, MOHP, Mansoura, 35711, Egypt
[f] Department of Basic Medical Sciences, College of Medicine, AlMaarefa University, Diriyah, P.O. BOX 71666, Riyadh, 11597, Saudi Arabia
[g] Department of Medical Biochemistry, Faculty of Medicine, Mansoura University, Mansoura, 35516, Egypt
[h] Pharmacognosy Department, Faculty of Pharmacy, Fayoum University, Fayoum, Egypt

ARTICLE INFO

Keywords:
Malabar tamarind
Antidiabetic
SARS-CoV-2 omicron
Antioxidant
Antibacterial
Guttiferones

ABSTRACT

Malabar tamarind tropical fruit, scientifically known as *Garcinia* gummi-gutta, is indigenous to Southeast Asia. In this work, the total methanolic extract of the Malabar fruit rind was examined by HPTLC fingerprinting, with quantitative evaluation of the total phenolics and flavonoids. Library of previously reported natural metabolites was utilized to demonstrate their affinity for specific target sites, they were evaluated against Omicron SARS-CoV-2 mainly it's Spike Protein, bacterial tyrosinase, and antidiabetic targets such α-glucosidase, pancreatic lipase and also α-amylase enzymes. The molecular docking revealed that the Guttiferone R possessed the highest binding affinity toward the Omicron Spike Protein with a stable binding mode, −8.67 kcal/mol binding energy and a 1.07 Å RMSD value compared to reference, Azithromycin, which has −8.90 kcal/mol binding affinity and a 1.20 Å RMSD value. On the other hand, the identified polyphenolic compounds; Vitexin, Prunin, Naringin, Hinokiflavone, Kaempherol-3-O-rutinoside, Gallic acid, Naringenin, and Catechin, showed remarkable antidiabetic activity by strong inhibitory activity against α-glucosidase and notable activity against α-amylase compared with acarbose as reference. According to antibacterial activity, the identified compounds showed low affinity with weak activity against screened bacterial strains. *In-vitro* evaluation of Tamarind antioxidant and antidiabetic potentials, it exhibited a free radical-scavenging potential with 71.75 % retardation and α-glucosidase, α-amylase and pancreatic lipase inhibitor activities with an IC50 of 391.3 ± 26.27, 95.03 ± 0.03 and 0.01043 ± 0.0004 μg/mL, respectively that emphasize the

* Corresponding author.
E-mail addresses: hbkhojah@ju.edu.sa (H. Khojah), emmoustafa@ju.edu.sa (E.M. Mostafa), 431205436@ju.edu.sa (A.A. Aljounaidi), abdo.saleh240@azhar.edu.eg (A.M. Saleh), mnablwai@um.edu.sa (M. El-Nablaway), ais03@fayoum.edu.eg (A. Ismail).

https://doi.org/10.1016/j.heliyon.2024.e35839
Received 4 April 2024; Received in revised form 29 June 2024; Accepted 5 August 2024
Available online 5 August 2024

molecular docking study. The findings imply that Malabar tamarind fruit rind possess antioxidant, antidiabetic, antibacterial and antiviral activities.

Abbreviations

HPTLC	High-Performance Thin Layer Chromatography
DPPH	2,2-Diphenyl-1-Picrylhydrazyl
RMSD	Root Mean Square Deviation
RCF	Relative Centrifugal Field
GAE	Gallic acid equivalent
RE	Rutin equivalent
RCSB	Research Collaboratory for Structural Bioinformatics
PDB	Protein Data Bank
ANOVA	Analysis of Variance
Rf	Retention Factor
MMFF94	Merck Molecular Force Field
IC50	Half Maximal Inhibitory Concentration

1. Introduction

The dicotyledonous Malabar Tamarind (*Garcinia cambogia* Roxb.) tree is indigenous to Sri Lanka, India, Malaysia and Africa. It is a member of the family of Guttiferae (Clusiaceae) (Fig. S1, Supplementary file). This native tropical plant is found in India and Southeast Asia. Its fruits are known for their sweet and sour flavor and for being used as a food supplement and for weight loss [1]. *Diabetes mellitus* is a worldwide chronic disease marked by abnormalities in the proteins, lipids, and carbohydrates metabolisms. It is brought on by a lack of insulin production, hyperglycemia, or both, and it can cause a number of metabolic changes that can be fatal to the patient [2]. Phenolic compounds as flavonoids, phenolic acids are naturally occurring in fruits and vegetables have piqued the interest of scientists recently due to their potential medical benefits and technological uses including their efficiency in treatment of diabetes [3]. Their multifaceted role in managing diabetes can be attributed to a number of mechanisms, including their antioxidant properties, which participate in reducing inflammation and oxidative stress, both of which are linked to the onset and progression of diabetes, improving insulin sensitivity by lowering the risk of insulin resistance, and by inhibiting glucose absorption by blocking the enzymes in the digestive system that break down carbohydrates [4,5]. Plants possessing potent antidiabetic enzymes inhibitors may be poisonous or carcinogenic, making them inappropriate for use in medicinal applications [6–9]. In other hand; The Omicron SARS-CoV-2 variant has expanded quickly, it is currently considered as one of the most common varieties all over the world, its characteristic feature is its capacity to resist against vaccinations or natural infections because of several spike protein mutations [10,11]. On the other side, alternative remedies involving medicinal herbs have been employed to mitigate specific COVID-19 symptoms. The SARS-CoV-2 development and sequential worldwide broadcast have brought about an unparalleled health emergency. The Omicron variant is the most recent variation to arise as the virus continues to change. Concerns have been expressed because of the high number of the Omicron variant's mutations, particularly in the Spike Protein [12]. The ability of virus SARS-CoV-2 to infect human cells is largely dependent on the Spike Protein. In order to create COVID-19 therapies and vaccinations that work, it is essential to comprehend the function and composition of the spike protein. The ultimate prevalent class of constituents present in the Guttiferae family plants, which involves genera like *Clusia, Hypericum*, and *Garcinia*, is called guttiferones. These substances have been the focus of a great deal of research lately and have a diverse range of biological actions. These are numerous polyisoprenylated benzophenones (PIBs), found in the tress of Malabar tamarind under study [13]. Garcinol is one of most well-known guttiferones in the rind of the Malabar Tamarind fruits. The fruits rind is rich in antioxidants and includes hydroxyl citric acid known as (HCA), thought to help with weight loss and fat burning [14]. Xanthochymol, another significant guttiferone, is present in *Hypericum perforatum* leaves. It is reported to have anti-oxidant, antibacterial, and anti-inflammatory potentials. It has also been found to have potential as an anti-cancer agent [15].

In this work, we first determined the total phenolics and flavonoids by quantitative means using the HPTLC fingerprint of the tamarind total methanolic extract. After that, a library of natural metabolites previously reported [16] in Tamarind fruit rind have been screened via *in silico* molecular docking for determination of their antidiabetic potential and also against both SARS-CoV-2 Omicron's Spike Protein and bacterial tyrosinase for determination of their antimicrobial activity and showing the affinity of the reported metabolites toward their targets site (Structures of active metabolites are collected in Fig. 1). The *in silico* field has emerged as a popular computational method used recently for biological screenings in a virtual manner, one can assess the estimated affinities and possible biological activities of a wide range of compounds, including natural, semisynthetic and synthetic compounds [17]. To ensure the computational results, three *in vitro* antidiabetic and antioxidant assays were conducted using the obtained data; Alpha-amylase inhibitor assay, alpha-glucosidase inhibitor assay, and pancreatic lipase inhibitor assay.

In conclusion, a variety of biological activities, including antioxidant, antidiabetic, and antiviral properties, have been proved in

the Guttiferae family plant members. Even though they have been used in traditional medicine for a variety of disorders and have the powers to be therapeutic agents, prospective researches are necessary for comprehension of their modes of action, efficacy and safety. Our goal is through an investigation into the Malabar Tamarind extract's potential as an antibacterial, antidiabetic, and antioxidant, up addition to filling up important knowledge gaps for the SARS-CoV-2 Omicron's Spike Protein type, this work offers encouraging new

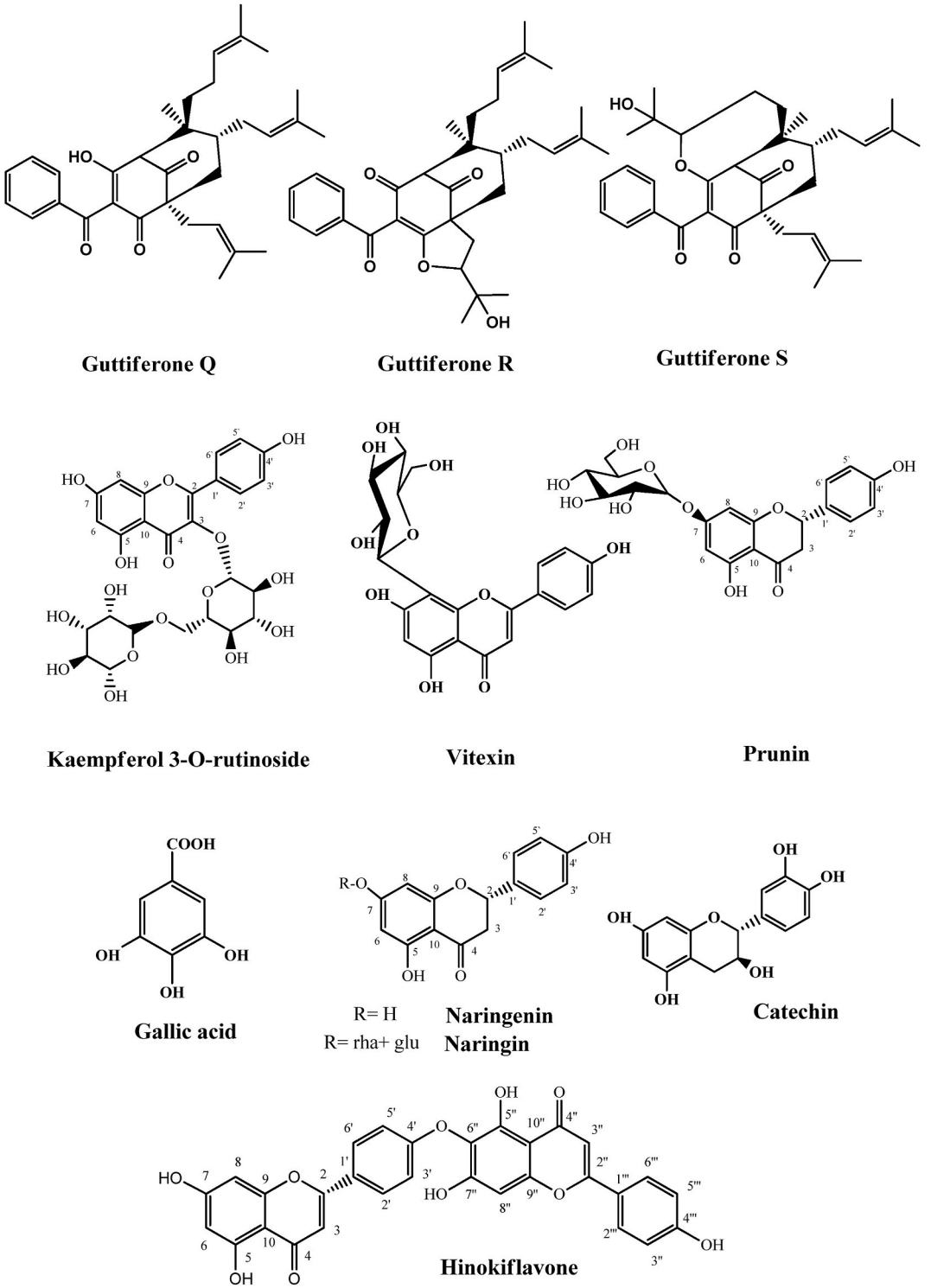

Fig. 1. Structures of active metabolites.

strategies for handling COVID-19 and its side effects. This study presents novel approaches with substantial implications for public health and clinical practice.

2. Materials and methods

1. Plant materials

Rinds of Malabar tamarind fruit were bought at a verified herbal market in January 2023 and verified in the Fayoum University in Taxonomy Department at the Faculty of Agriculture and stored in the Department of Pharmacognosy, Faculty of Pharmacy, Fayoum University with a voucher sample ID (No. FuPD-58).

2. Preparation of extracts

A weighted amount of 50 g of the Malabar tamarind rind was cleaned, grounded using a Moulinex grinder set to 3000 RCF for 6 min at room temperature to create a homogenized powder. About 2.65 g of dried total extract were produced by cold macerating the resultant powder in 70 % methanol and then vacuum-pressurizing the mixture to evaporate at 40 °C. The extract was employed for investigations pertaining to both phytochemistry and biology.

3. HPTLC Fingerprinting

After being weighted and diluted in methanol at a concentration of 6 mg/mL, the Malabar Tamarind crude methanolic extract sample was filtered. Following that, nitrogen flow was used to apply the filtered solutions. The following operational conditions have been carried out; The rate of syringe delivery is 10 s μL-1 (100 nL s-1) and its injection volume is 2 μL to apply sample band of 6 mm width, with 15 mm distance from the bottom.

Software of WinCATS, (CAMAG, Muttenz, version 1.4.1, Switzerland), is operating CAMAG TLC Scanner 4, which is configured in the absorbance technique. The radiation source was a tungsten bulb and Deuterium.

Densitometric analysis was performed on chromatograms at 280, 254, and 365 nm (1 nm). The chromatographic separation was performed in an automated development chamber (ADC2, CAMAG) that was saturated with 33 % relative humidity using HPTLC plates (silica gel 60 F254, 10*20 cm).

4. Total flavonoid and phenolic contents determination

Ultrasonic bath was utilized for extracting the weighed Tamarind rind powder (0.5 g) for 20 min. Then, the extract was filtered, and the volume of the filtrate was completed to reach 50 mL by methanol. After that, samples aliquots were prepared and assays were repeated twice.

4.1 Total phenolics content

Total phenolics content has been assessed using the Folin-Ciocalteu technique. Gallic acid was serially diluted multiple times (20, 40, 60, 80, and 100 mg/L) to generate a standard curve (Fig. S2, Supplementary file). Nine milliliters of distilled water and 1 mL of the tested extract were added to gallic acid solutions in a 25 mL volumetric flask. Ten milliliters of Na_2CO_3 (7 %) and 1 mL of reagent of Folin-Ciocalteu were added after 5 min. The resulted solution was further thoroughly mixed, the volume was completed to 25 mL using room-temperature distilled water, and it was left to sit for 90 min. With one milliliter of pure water, a blank experiment was run. The absorbances at 750 nm were recorded using a UV-VIS spectrophotometer. Using the standard curve, the total phenolic content of each sample was calculated and represented as reported [mg of gallic acid equivalent (GAE)/100 mg dry weight] [18].

4.2 Total flavonoids content

A colorimetric assay using aluminum chloride has been performed to measure the total flavonoid concentration. Initially, as shown in (Fig. S3, Supplementary file), plotting the standard curve using different standard rutin concentrations in the order of (20, 40, 60, 80, and 100 mg/L). Then, to 10 mL volumetric flask containing already distilled water (4 mL), one ml of each of tested sample and the prepared standard solution were added together. Afterwards, 0.3 mL of $NaNO_2$ (5 %) was added, and the combination was mixed with 0.3 mL of $AlCl_3$ (2 %), after 5 min. After leaving it for 6 min, 2 mL of 1M NaOH were added. Distilled water was used to adjust the volume to 10 mL, and the mixture was thoroughly mixed. At 510 nm, the absorbance was measured in relation to a blank solution made with 1 mL of distilled water. The standard curve was used to calculate the total flavonoids content. [19], In the control experiment, 1 mL of distilled water was used.

As reference samples, rutin and gallic acid standards (E. Merk, Germany), were obtained. UV spectra were recorded using UV–visible spectrophotometer (Shimadzu UV-1650), which measures absorbance in the UV spectrum.

5. Free radicle Scavenging potential determination

Using 2,2-Diphenyl-1-picrylhydrazyl, the 70 % methanol extracts of Malabar tamarind fruit rinds were evaluated for their capacity to scavenge free radicals according to Ref. [20]. In a 96-well plate, a triplicate of concentration of total tamarind methanolic extract (1 mg/mL), was produced in aliquots. The reaction was performed using the reaction mixture consisting of 190 μl of DPPH solution and 10 μl of the sample, which produced a final volume of 200 μl and a DPPH concentration of roughly 300 μM. Ten μl of methanol were used to process a second blank experiment. Following a 30-min incubation period at 30 ± 1 °C, measuring the absorbance at 517 nm wavelength and allowing for the calculation of the percentage of inhibition of oxidation.

6 Alpha-amylase inhibitor assay

The sample was prepared in methanol at final concentrations of 25, 50, 125, 250, and 500 μg/mL, whereas the Acarbose stock solution was prepared at final concentrations of 1548.94, 154.894, 15.4894, 0.154894, and 0.0154894 μg/mL. In short, the assay was performed using [21] method, which involved mixing 140 μL of phosphate buffer (50 mM, 0.9 % NaCl, PH = 7) with 20 μL of samples or blank per 96-microwell plate. After adding 20 μL of the amylase enzyme to the mixture, it was incubated at 37 °C for 15 min. After adding 20 μL of 0.375 mM substrate in phosphate buffer, the resulting mixture was once again incubated at 37 °C for 10 min. Using a microplate reader (Onega, USA), the *p*-nitroanilline release from the substrate was measured at 405 nm to evaluate the enzyme activity. The following equation was used to compute the percentage of α-amylase inhibition: % Inhibition = [(A blank – A sample)/A blank] x 100.

7. Alpha-glucosidase inhibitor assay

Sample was prepared at the following final concentrations in methanol: 1000, 500, 250, 125, and 100 μg/mL and Acarbose stock solution of 2 mM in phosphate buffer (100 mM, PH = 7) was created, and the following final concentrations were prepared in water: 250, 125, 62.5, 31.25, and 15.625 μg/mL. In 96-microwell plates, a 10-min incubation period was conducted at 37 °C with 25 μL (samples and blank) and 50 μL of *Saccharomyces cerevisiae* α-glucosidase (0.3 U/mL) in phosphate buffer (0.1 M, pH 7). This procedure was followed in accordance with the approach of [22]. Subsequently, a mixture containing 25 μL of 3 mM para nitrophenyl β-D-glucopyranoside (pNPG) was added and incubated for an additional 5 min at 37 °C using a microplate reader (Onega, USA), In order to measure the enzyme activity, the release of *p*-nitrophenol from the pNPG substrate was detected at 405 nm. The formula was utilized for determination is; % Inhibition = [(A blank – A sample)/A blank] x 100.

8. Pancreatic lipase inhibitor assay

Sample was prepared at the concentration of 500, 250, 125, 50 and 25 μg/mL in methanol while Orlistat standard positive control compound concentrations were prepared: 1000, 100, 10, 1, and 0.1 nM, starting with a stock solution of 2 μM in methanol. Briefly stated, the experiment was performed using [22] method, which involved adding 25 μL of samples or blank to 110 μL of Tris buffer (100 mM PH = 8) on 96-microwell plates. Next, 50 μL of procine lipase (1 mg/mL) was added, and the mixture was incubated at 37 °C for 10 min. After that, 10 μL of para 4-nitrophenyl dodecanoate (*p*-NPD) was added to the reaction, and it was incubated for 20 min at 37 °C. Using a microplate reader (Onega, USA), pNDP substrate released *p*-nitrophenol, which further measured at 405 nm to evaluate the enzyme activity. The following equation was used to compute the percentage of lipase inhibition: % Inhibition = [(A blank – A sample)/A blank] x 100.

9. Molecular docking study

A popular and effective tool for virtual biological screening is the computational (*in silico*) approach. This approach has been used to assess the biological activities and determined affinities of synthetic, semisynthetic, and natural materials [17]. To demonstrate the compounds' affinity for the spike protein of SARS-CoV-2 Omicron, α-amylase, α-glucosidase, pancreatic lipase, and bacterial tyrosinase, a library of natural metabolites was screened in this work. Firstly, proteins had been obtained from the data bank of proteins (PDB), provided by RCSB (protein Ids: 7T9K, 1lpb, 6gxv, 3w37, and 3nq1). In order to create the targeted proteins, water molecules were eliminated, incomplete valence atoms were filled in, absent amino acids were added, and the energy of protein peptide was minimized by the aid of CHARMM force fields [23]. After selection, the essential amino acids were prepared for screening. Drawing the studied chemicals in two dimensions was processed by Chem-Bio Draw Ultra ver. 17.0 with file format in SDF. After protonating the tested ligands, the force field of MMFF94 with 0.1 RMSD kcal/mol was used to reduce their energy. After that, the minimized structures were kept for use in molecular docking. Each molecule was able to construct twenty various interaction poses with the protein during the refining phase utilising docking algorithms. The histone deacetylase active site's best-fit positions were rated for docking (affinity interaction energy). To build the 3D orientation, a program called Discovery Studio 2016 visualizer was utilized [12].

10. Statistical analysis

One-way ANOVA was used to analyse the biochemical data, which were shown as means ± SE. Duncan's multiple range tests and the least-significant difference test were used to compare the means across the groups. According to Graph Pad Prism 5, statistical significance was shown by a P-value of less than 0.05.

3. Results

1. HPTLC Fingerprinting

From Fig. 2 and (Fig. S4, Supplementary file), it is evident that the produced chromatogram of the Malabar tamarind methanol extract, when scanned at various wavelengths, has a minimum of 8 unique components. The maximum Rf values that were found to be most common at 280 nm were 0.21, 0.31, 0.42, 0.5, 0.52, 0.62, 0.71, and 0.77, with corresponding percentage areas of 43.64 %, 6.23 %, 2.29 %, 3.74 %, 5.94 %, 30.8 %, 5.48 %, and 1.88 %. The remaining compounds are fewer in number. Consequently, the chromatogram produced will be accurate when using the selected solvent system of (Phenol: Acetone: Formic acid, 16.5:75: 8.5), which makes it an excellent technique for tamarind extract fingerprinting.

2. Total flavonoid and phenolic contents determination

The tamarind methanolic total extract was quantitavely investigated for both its total phenolics content and flavonoids using gallic acid and aluminum chloride assay, respectively. The total phenolics were evaluated using the Folin-Ciocalteu method, while the flavonoids were measured by the rutin equivalent [20]. The concentrations of both flavonoid and total phenolic contents in tamarind investigated samples are inferred from their standard curves and are expressed as mg of rutin and gallic acid equivalents, or (RE)/100 mg and (GAE)/100 mg dry wt., respectively.

The total flavonoids and phenolic contents were 79.45 mg/g and 46.99 mg/g, respectively, according to the results. The quantitative analysis yielded results that are represented collectively by Fig. S5 histogram (Supplementary file).

3. *In silico* molecular docking

3.1. *Inhibition of SARS-CoV-2 OMICRON spike protein*

Proteins with the following IDs were downloaded: 7T9K, 1lpb, 6gxv, 3w37, and 3nq1. Protein and its metabolites were created, and MMFF94 force field was used to reduce energy. After the finishing the molecular docking, Table 1 was constructed, affinity scores and RMSD values were collated, twenty poses were created, and the ideal orientations were photographed. The reference molecule, azithromycin, possessed Pi-Alkyl five interactions with Lys856, Pro589, Leu966, and Met740. In addition, it produced three hydrogen bond interactions with Lys856, Asn978, and Cys743 at distances of 2.62, 1.82, and 2.35 Å. Additionally, there was an ionic attractive contact between the cationic NH group and Asp745. (Supplementary file, Fig. S6).

In guttiferone-Q, eleven Pi-alkyl and Pi-sigma interactions with Pro589, Lys856, Val976, Arg319, Leu966, Pro322, Cys538 and Cys590, were predicted. Furthermore, 2 H-bonds with 2.06 and 2.68 Å lengths are forming a binding between it and Asp745 and Thr549. The Omicron Spike Protein-guttiferone Q complex's total binding energy was found to be −8.56 kcal/mol, while the reference compound's was −8.90 kcal/mol (Supplementary file, Fig. S7).

The binding energy of the guttiferone-R binding mode against the target site of Spike Protein was −8.67 kcal/mol. In addition, four Pi-Alkyl interactions between guttiferone-R and Pro589, Ile587, Leu546, and Leu966 were created. Three H-bonds with lengths of 2.44, 2.59, and 2.25 Å were used by guttiferone-R to connect with Leu977, Lys856, and Asp571 (Fig. 3).

The binding energy of the guttiferone-S binding mode against the target site of Spike Protein was −8.55 kcal/mol. Asp745, Asn978, Leu977, and Arg1000 are connected to guttiferone-S through four hydrogen bonds, each measuring 1.94, 2.54, 2.56, and 2.37 Å in

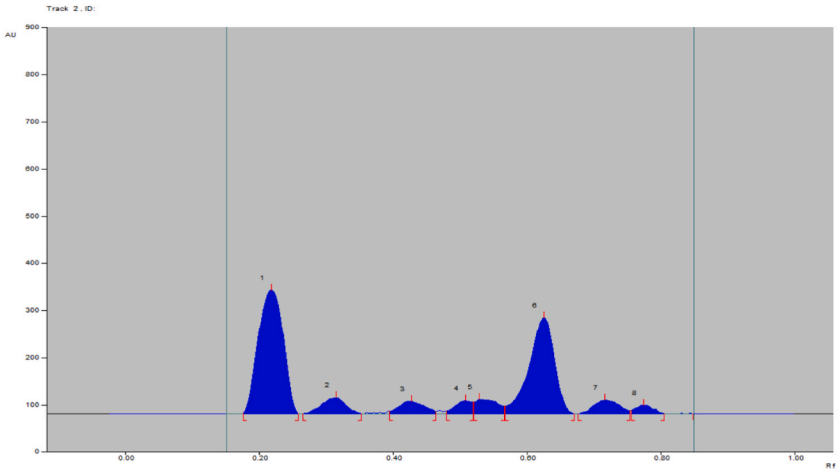

Fig. 2. HPTLC Finger print of total methanolic extract of Malabar Tamarind at 280 nm.

Table 1
(DG, RMSD, interactions) kcal/mol of (tested ligands) against targeted sites.

Targets screened	Tested compounds	RMSD value (Å)	Docking (Affinity) score (kcal/mol)	Interactions	
				H.B	Pi -interaction
Omicron Spike Protein	Guttiferone-Q	1.37	−8.56	2	11
	Guttiferone-R	1.07	−8.67	3	4
	Guttiferone-S	1.21	−8.55	4	2
	Azithromycin	1.20	−8.90	3	5
α-glucosidase	Vitexin	1.65	−9.68	5	5
	Prunin	1.09	−10.02	6	6
	Naringin	1.23	−10.36	5	6
	Acarbose	1.01	−11.54	12	4
α-amylase	Prunin	1.25	−9.67	7	5
	Hinokiflavone	1.07	−9.64	3	5
	Kaempherol3-O-rutinoside	1.14	−9.56	5	8
	Acarbose	1.13	−10.25	12	3
Pancreatic lipase	Prunin	1.38	−6.90	1	3
	Co-crystalized ligand	1.03	−6.23	2	0
Bacterial tyrosinase	Gallic acid	1.07	−6.01	1	2
	Naringenin	1.24	−6.35	2	3
	Catechin	1.31	−7.12	3	4
	kojic acid	1.07	−5.63	1	2

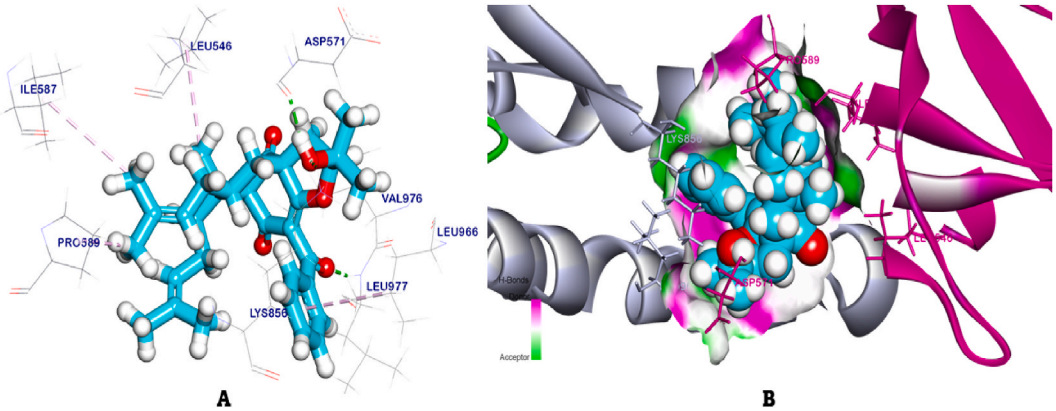

Fig. 3. 3D and surface mapping of Guttiferone-R (Fig. a, b) against Omicron Spike Protein.

length. Moreover, engaged with Leu966 and Val976 by two Pi-alkyl interactions (Supplementary file, Fig. S8).

3.2. Antibacterial activity (bacterial tyrosinase inhibition)

The co-crystalized ligand (kojic acid) binding mode exhibited an energy of binding −5.63 Kcal/mol against bacterial tyrosinase (Fig. S9, supplementary file). It formed one hydrogen bond and two hydrophobic π-interactions with Gly200, Arg209 and Pro201, respectively.

The binding mode of Gallic acid, naringenin, and Catechin showed an energy binding of −6.01, −6.35 and −7.12 Kcal/mol against the bacterial tyrosinase. **Gallic acid** formed two hydrophobic π-interactions and two metal ion interactions with His208, Val218, CU501 and CU502. Furthermore, it showed one H-bond with Met215 (distance of 2.06 Å, Fig. S10, supplementary file). **Naringenin** interacted with Arg202, and Met215 by 2 hydrogen bonds accompanied by distances of 2.33, and 2.37 Å, moreover, formed three hydrophobic π-interactions and two metal ion interactions with His208, Val218, Phe197, CU501 and CU502 (Fig. S11, supplementary file). **Catechin** showed the highest affinity with bacterial tyrosinase by forming three H-bonds with Met215, Gly216, and Glu158 with distances of 2.28, 2.44, and 2.51 Å. additionally, forming four hydrophobic π-intera-ctions and two metal ion interactions with Pro201, His208, Val218, Arg209, CU501 and CU502 (Fig. 4).

3.3. Anti-diabetic activity

The reference compound (acarbose) exhibited binding energies of −11.54 and −10.25 kcal/mol against the α-glucosidase and α-amylase target sites, respectively (Figs. S12 and S13 in supplementary file). It formed four hydrophobic π-interactions with Met470, Trp432, Trp329, and Phe601 against α-glucosidase and three hydrophobic π-interactions with Met109, Ala338, and Leu339 against

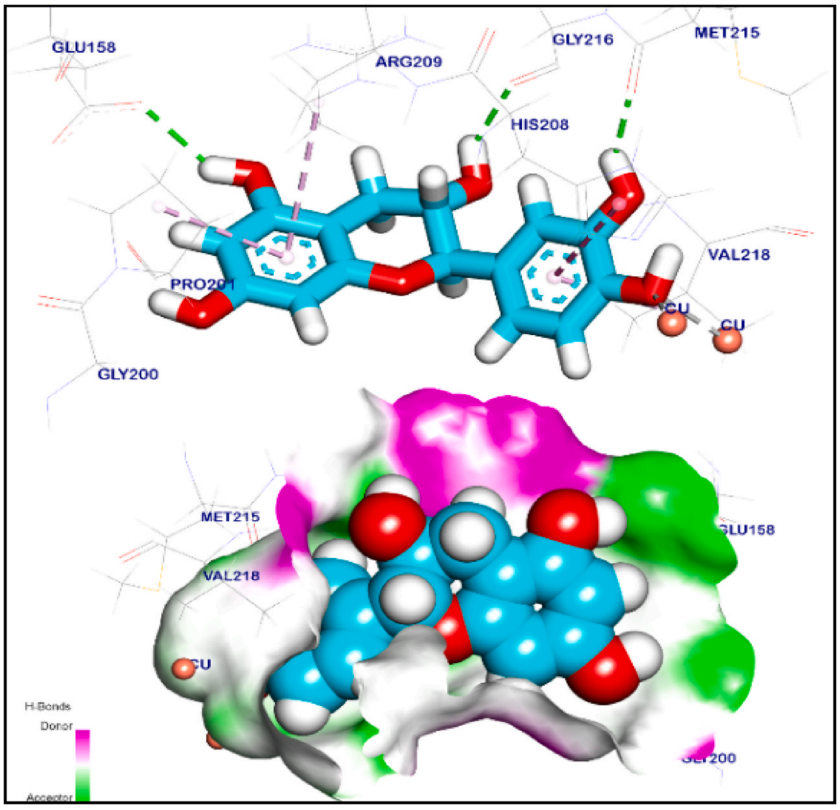

Fig. 4. 3D and surface mapping of Catechin against bacterial tyrosinase.

α-amylase, additionally interacting with Asn237, Ala234, ASsp232, Arg552, Asp357, His626, and Asp568 by twelve hydrogen bonds against α-glucosidase and formed twelve hydrogen bonds against α-amylase with Gln51, His331, Asp332, Arg232, Asp234, Glu265, His238, Lys237, Glu192, and Asp166.

3.3.1. *α-glucosidase inhibition*

Vitexin binding mode exhibited a binding energy of −9.68 kcal/mol toward the α-glucosidase target site. It's formed five hydrophobic π-interactions with Asp568, Met470, Ala602, and Ala628. Additionally, Vitexin interacted with Asp630, Met470, Trp432, Asp357, and Asp469 by five hydrogen bonds with distance ranges of 1.81–2.69 Å (Fig. S14, supplementary file). **Prunin** binding mode exhibited a binding energy of −10.02 kcal/mol against the α-glucosidase target site. Prunin formed six hydrophobic π-interactions with Trp329, Asp568, and Lys506, moreover, interacted with Ala234, Lys506, His626, Asp568, and Asp357 by six H-bonds with 1.94–2.88 Å distance ranges (Fig. S15, supplementary file). **Naringin** showed a binding energy of −11.54 kcal/mol against the α-glucosidase target site. It formed six hydrophobic π-interactions with Met470, Ile358, Trp432, Trp329, Ala602, and Ala628. Additionally, Naringin interacted with Asp232, Asp357, Asp469, and Glu603 by five hydrogen bonds with distance ranges of 1.74–2.71 Å (Fig. 5).

3.3.2. *α-amylase inhibition*

Prunin binding mode exhibited a −9.67 kcal/mol binding energy against the α-amylase target site. Prunin formed five hydrophobic π-interactions with Ala235, Leu199, Tyr58, and Met200. Additionally, Prunin showed seven hydrogen bonds with Asp332, His331, Arg232, Met200, and Tyr58 with distance ranges of 2.43–3.07 Å (Fig. 6). While, binding mode of **Hinokiflavone** has a binding energy of −9.64 kcal/mol. Hinokiflavone formed five hydrophobic π-interactions with Ala235, Glu265, Tyr58, and Met200, moreover, interacted with Glu192, Lys237, and Asp332 by three H-bonds with 2.07–2.60 Å distance ranges of (Fig. S16, supplementary file). **kaempferol 3-O-rutinoside** exhibited a binding energy of −9.56 kcal/mol against the α-amylase target site. It formed eight hydrophobic π-interactions with Ala235, Leu339, Tyr58, Asp234, Trp15 and Met200. Additionally, kaempferol 3-O-rutinoside interacted with Glu192, Glu265, Asp234, and Asp332 by five H-bonds with 2.13–2.60 Å distance ranges (Fig. S17, supplementary file).

3.3.3. *Pancreatic lipase inhibition*

Binding energy of the pancreatic lipase co-crystalized ligand exhibited of −6.23 kcal/mol. It was showed interacting with Phe77 and Leu153 with two H-bonds (distance of 2.16, and 2.45 Å, Fig. S18, supplementary file). The binding mode of **Prunin** exhibited a binding energy of −6.90 kcal/mol against Pancreatic lipase target site. Prunin formed three hydrophobic π-interactions with Phe77, Phe215, and Tyr114. Additionally, Prunin showed one hydrogen bond with Ser152 with distance of 2.71 Å (Fig. 7).

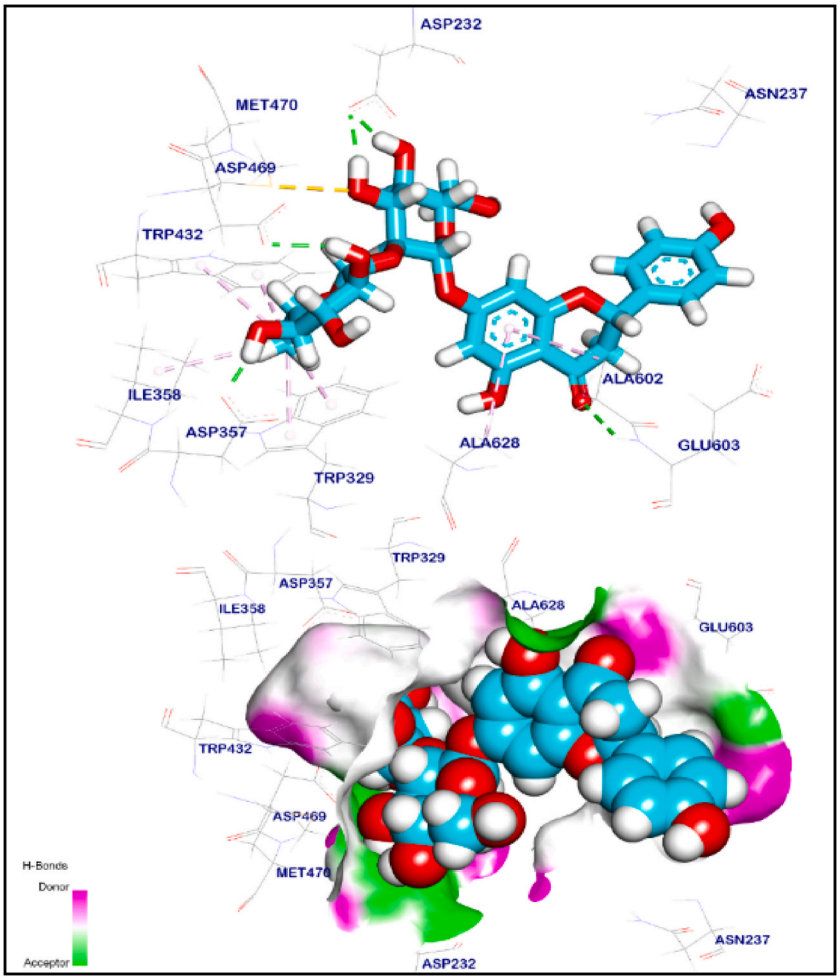

Fig. 5. 3D and surface mapping of Naringin against α-glucosidase.

All of the tested ligands' interactions with the targeted locations and the RMSD results are summarised in (Table 1).

4. In vitro evaluation of antioxidant and antidiabetic activities

4.1. Free radical-scavenging activity

A quick, easy, and practical way to check materials for radical scavenging activity is to use the DPPH photometric assay. Because of these benefits, it's the perfect tool for choosing natural extracts or substances that may have antioxidant qualities for use in products. This assay's approach relies on antioxidants' capacity to couple with the DPPH radical's odd electron, bleaching its absorption in the process. It is necessary to have a hydrogen-donating group, like hydroxyl, and because of this structural requirement, phenolics are frequently present in plant extracts [24].

Compared to the control substance, rutin (87.9 %), the total methanolic extract of Tamarind rind demonstrated a lower level of antioxidant activity (71.75 % inhibition). This discrepancy could be explained by *Garcinia cambogia* Roxb's increased phenolic content. This observation might be the result of the extract's high phenolic content, [25]. Results are depicted in Fig. S19, supplementary file.

4.2. Antidiabetic activity

4.2.1. Alpha-glucosidase inhibitor activity

The finding was found that tamarind extract exhibited an inhibitory activity with an IC50 of 223.8 ± 5.86 μg/mL. The Acarbose has an IC50 of 95.03 ± 0.03 μg/mL (Fig. 8).

4.2.2. Alpha-amylase inhibitor activity

The α-amylase inhibitor activity of tamarind extract was assessed (Fig. 9). For all concentrations examined, the percentage of

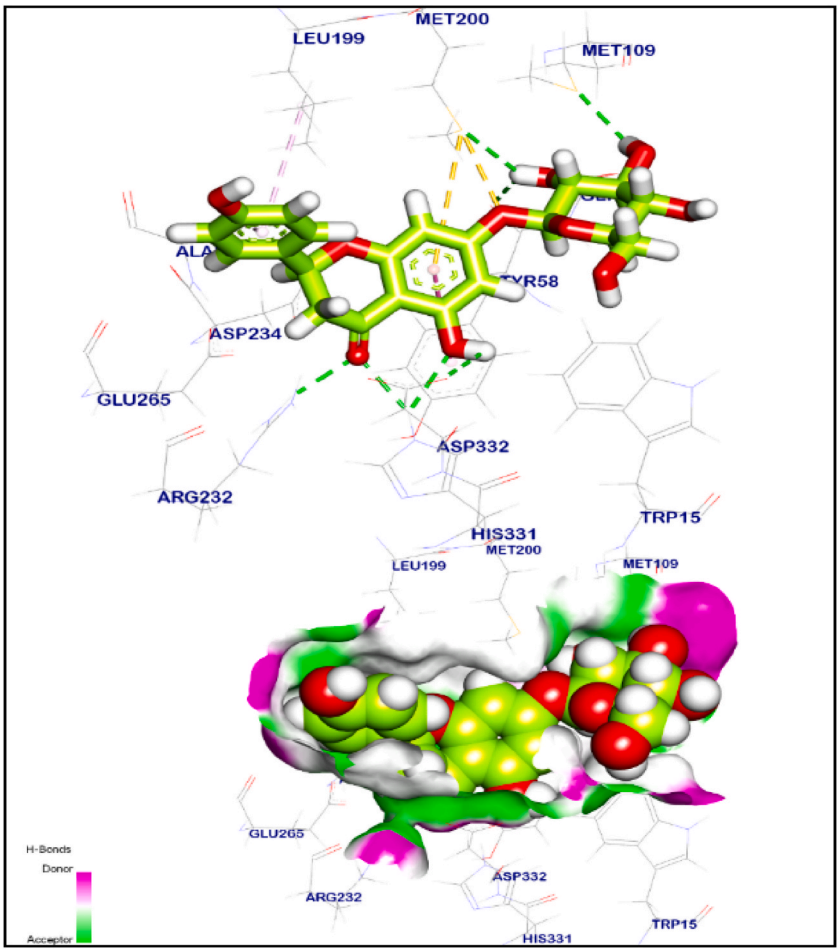

Fig. 6. 3D and surface mapping of Prunin against α-amylase.

inhibitor activity has a dose-dependency increase. Acarbose is used as a standard positive control compound. The values are the average of triplicate experiments and are expressed as mean ± SE of the mean. The finding was found that tamarind extract exhibited an inhibitory activity with an IC50 of 391.3 ± 26.27 μg/mL. The Acarbose has an IC50 of 1.863 ± 0.1 μg/mL.

4.2.3. Pancreatic lipase inhibitor activity

The pancreatic lipase inhibitor activity of tamarind extract was assessed (Fig. S20, supplementary file). For all concentrations examined, the percentage of inhibitor activity increased in a dose-dependent manner. Orlistat is used as a standard positive control compound. Triplicate experiments's average values are expressed as mean ± SE of the mean. The finding was found that tamarind extract exhibited weak inhibitor activity with an IC50 of more than 500 μg/mL. The Orlistat has an IC50 of 0.01043 ± 0.0004 μg/mL.

In summary; Malabar tamaraind is a promising natural source of different phenolic compounds such as flavonoids, catechins and phenolic acids. Firstly by fingerprinting the extract by HPTLC profiling of its contents, it reveals presence of various phenolic compounds, followed by performing quataitative assay which records its total flavonoids and phenolic contents (79.45 mg/g and 46.99 mg/g, respectively). Then, Tamarind's antioxidant and antidiabetic potentials were assessed *in vitro* and results showed that it could scavenge free radicals with a 71.75 % inhibition and also inhibit the activities of α-glucosidase, α-amylase, and pancreatic lipase with IC50 values of 391.3 ± 26.27, 95.03 ± 0.03, and 0.01043 ± 0.0004 μg/mL, respectively. These findings highlight the molecular docking study by its α-glucosidase, α-amylase, and pancreatic lipase inhibitor activities, with IC50 values of 391.3 ± 26.27, 95.03 ± 0.03, and 0.01043 ± 0.0004 μg/mL, respectively, and also when compared to the reference drug azithromycin, guttiferone R had the highest binding affinity for the Omicron Spike Protein, exhibiting a stable binding mode, −8.67 kcal/mol binding energy, and a 1.07 Å RMSD value. Regarding antibacterial study, limitation of the current study lies into testing plant extract against broad spectrum microbial strains, the point that will put in consideration in our future researches. The overall results suggest that the rind of the Malabar tamarind fruit has antiviral, antibacterial, antidiabetic, and antioxidant properties.

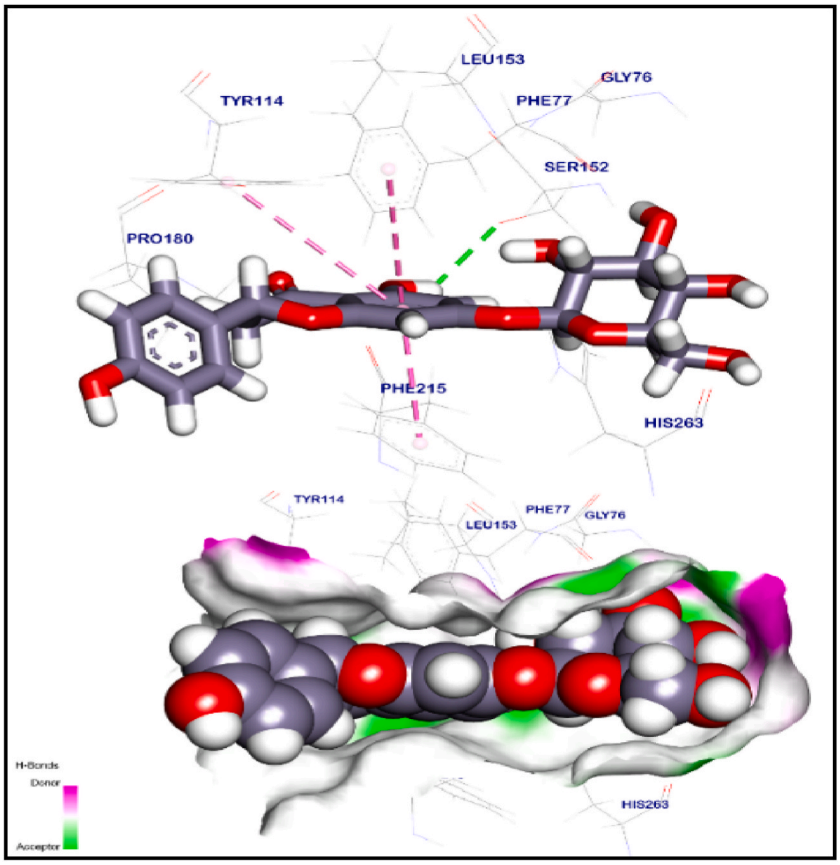

Fig. 7. 3D and surface mapping of Prunin against Pancreatic lipase.

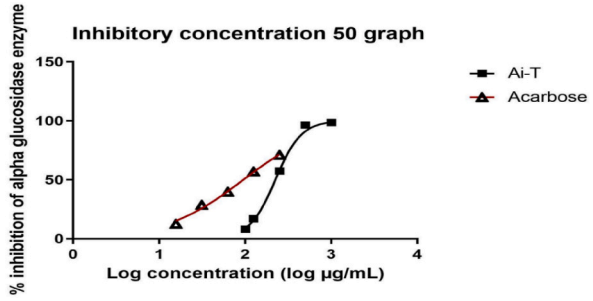

Fig. 8. Alpha-glucosidase inhibitor activity of tamarind extract. Data are presented as Mean ± SE (n = 3).

5. Discussion

The current study is considered the first report of SARS-Cov-2 Omicron Spike Protein, antibacterial, antidiabetic potentials evaluation by molecular docking alongside *in vitro* evaluation of antidiabetic and antioxidant potentials of Malabar Tamarind extract as well as its prospective therapeutic advantages. Firstly, HPTLC screening detected presence of polyphenols and flavonoids components which confirmed by quantitave assays for estimation of their contents, which in consequense, gave a prediction for Tamaraind potency as antioxidant, antiviral for SARS-CoV-2 Omicron, antibacterial and also antidiabeic agent. *In vitro* evaluation of antioxidant and antidiabetic activities served this prediction, which encouraged us to perform an in-silico molecular docking study. Based on docking data, the most binding affinity appears to be for guttiferone-R, which point to a stable binding state, guttiferone-R appears to have the greatest potential as a therapeutic candidate. Even though their greater RMSD values point to a less stable binding mode and the requirement for additional research, guttiferones Q and S might also have potential. Because of its well-known binding affinity, azithromycin is employed as a reference in the study and can be used to compare and verify the outcomes of the other drugs. Even

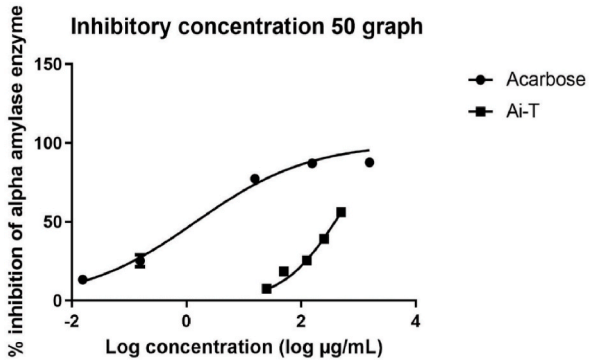

Fig. 9. Alpha-amylase inhibitor activity of tamarind extract. Data are presented as Mean ± SE (n = 3).

though guttiferones may have therapeutic benefits, additional investigation is required to completely comprehend guttiferone modes of action as well as to assess guttiferone safety and efficacy in humans. Furthermore, another constituent exhibited noteworthy antidiabetic effects by acting as a competitive and reversible inhibitor targeting α-amylase and α-glucosidase. This action leads to the delayed digestion of sugars in the gut, consequently causing a significant reduction in postprandial glucose and insulin levels. Naringin, prunin were the most tested flavonoids with binding affinity to target sites in the antidiabetic assays which matched recent studies about their roles in diabetes management [26,27], Regarding the antibacterial screening; it was highlighted around the tyrosinase enzyme inhibition as it is known that bacterial tyrosinases have a critical role in bacterial biosynthetic pathway [28], and its inhibition is the main core of any selective antibacterial drug [29]. In our study, catechin possessed the highest affinity against bacterial tyrosinase which matches a previous record in this area [28]. The testing of plant extract against broad spectrum microbial strains is the current study's limitation, which will be taken into account in our upcoming investigations.

Clinical implications and impact on treatment; Comprehending mechanisms finding out how the Omicron Spike Protein interacts with host cells can help in the creation of antiviral medications and vaccinations that work better. Understanding Spike Protein mutations can also aid in anticipating and reducing the likelihood of immune-evading escape variants. These discoveries may result in the development of small molecule inhibitors or tailored monoclonal antibodies that selectively neutralize the Omicron variety, thereby enhancing the prognosis of patients with infection. The identification of compounds connected to the Omicron Spike Protein that possess antibacterial qualities could result in the creation of novel antibacterial agents. Combining antiviral and antibacterial medications could be a strategic approach to controlling COVID-19, especially in severe instances where bacterial superinfections are widespread. This could be especially helpful in treating secondary bacterial infections in COVID-19 patients.

The *in vitro* assessment demonstrating antidiabetic potentials implies that Tamarind under investigation could be useful in controlling blood glucose levels. For COVID-19 patients with diabetes, who are more likely to experience severe consequences, this is especially important. Patients with diabetes may benefit from include the extract in their treatment plans due to its ability to control blood glucose levels. As an adjunctive treatment, clinicians may suggest Malabar Tamarind. Using Malabar Tamarind extract to reduce oxidative damage may be beneficial to general health. Practical recommendation for clinicians to include antiviral and antibacterial tactics in individualized treatment plans; inform patients about the advantages and possible applications of natural supplements, such as Malabar Tamarind extract, in health management.

Data availability statement

All data are included in the manuscript, any additional information needed, contact the corresponding author.

Funding

This work was not supported by any funding.

CRediT authorship contribution statement

Hanan Khojah: Validation, Supervision, Methodology. **Ehab M. Mostafa:** Writing – original draft, Supervision, Software. **Asail A. Aljounaidi:** Writing – original draft, Methodology. **Abdulrahman M. Saleh:** Visualization, Validation, Methodology, Data curation. **Mohammad El-Nablaway:** Methodology. **Ahmed Ismail:** Writing – review & editing, Writing – original draft, Validation, Supervision, Methodology, Investigation, Data curation, Conceptualization.

Declaration of competing interest

The authors declare that they have no known competing financial interests or personal relationships that could have appeared to influence the work reported in this paper.

Acknowledgements

Not applicable.

Appendix A. Supplementary data

Supplementary data to this article can be found online at https://doi.org/10.1016/j.heliyon.2024.e35839.

References

[1] W. Sergio, A natural food, the malabar tamarind, may be effective in the treatment of obesity, Med. Hypotheses 27 (1) (1988) 39–40.
[2] D. de Paulo Farias, et al., Antidiabetic potential of dietary polyphenols: a mechanistic review, Food Res. Int. 145 (2021) 110383.
[3] F.F. de Araújo, et al., Polyphenols and their applications: an approach in food chemistry and innovation potential, Food Chem. 338 (2021) 127535.
[4] J.A. Scott, G.L. King, Oxidative stress and antioxidant treatment in diabetes, Ann. N. Y. Acad. Sci. 1031 (1) (2004) 204–213.
[5] A. Podsedek, et al., In vitro inhibitory effect on digestive enzymes and antioxidant potential of commonly consumed fruits, J. Agric. Food Chem. 62 (20) (2014) 4610–4617.
[6] C. Fennell, et al., Assessing African medicinal plants for efficacy and safety: pharmacological screening and toxicology, J. Ethnopharmacol. 94 (2–3) (2004) 205–217.
[7] J.O. Unuofin, G.A. Otunola, A.J. Afolayan, In vitro α-amylase, α-glucosidase, lipase inhibitory and cytotoxic activities of tuber extracts of Kedrostis africana (L.) Cogn, Heliyon 4 (9) (2018) e00810.
[8] Y. Gu, et al., Inhibition of key digestive enzymes by cocoa extracts and procyanidins, J. Agric. Food Chem. 59 (10) (2011) 5305–5311.
[9] S.S. Nair, V. Kavrekar, A. Mishra, In vitro studies on alpha amylase and alpha glucosidase inhibitory activities of selected plant extracts, Eur. J. Exp. Biol. 3 (1) (2013) 128–132.
[10] H.M. Mengist, et al., Mutations of SARS-CoV-2 spike protein: implications on immune evasion and vaccine-induced immunity, in: Seminars in Immunology, Elsevier, 2021.
[11] W.T. Harvey, et al., SARS-CoV-2 variants, spike mutations and immune escape, Nat. Rev. Microbiol. 19 (7) (2021) 409–424.
[12] E.F. El Azab, et al., New insights into geraniol's antihemolytic, anti-inflammatory, antioxidant, and anticoagulant potentials using a combined biological and in silico screening strategy, Inflammopharmacology 30 (5) (2022) 1811–1833.
[13] S. Kumar, S. Sharma, S.K. Chattopadhyay, The potential health benefit of polyisoprenylated benzophenones from Garcinia and related genera: ethnobotanical and therapeutic importance, Fitoterapia 89 (2013) 86–125.
[14] H. Baky M., H. Fahmy, M.A. Farag, Recent advances in Garcinia cambogia nutraceuticals in relation to its hydroxy citric acid level. A comprehensive review of its bioactive production, formulation, and analysis with future perspectives, ACS Omega 7 (30) (2022) 25948–25957.
[15] S. Kumar, et al., Cytotoxic activities of xanthochymol and isoxanthochymol substantiated by LC-MS/MS, Planta Med. 73 (14) (2007) 1452–1456.
[16] H.Y. Aati, et al., Garcinia cambogia phenolics as potent anti-COVID-19 agents: phytochemical profiling, biological activities, and molecular docking, Plants 11 (19) (2022) 2521.
[17] I.H. Eissa, et al., Ligand and structure-based in silico determination of the most promising SARS-CoV-2 nsp16-nsp10 2′-o-Methyltransferase complex inhibitors among 3009 FDA approved drugs, Molecules 27 (7) (2022) 2287.
[18] N. Siddiqui, et al., Spectrophotometric determination of the total phenolic content, spectral and fluorescence study of the herbal Unani drug Gul-e-Zoofa (Nepeta bracteata Benth), Journal of Taibah university medical sciences 12 (4) (2017) 360–363.
[19] M.H. Hetta, et al., In-vitro and in-vivo hypolipidemic activity of spinach roots and flowers, Iran. J. Pharm. Res. (IJPR): Int. J. Psychol. Res. 16 (4) (2017) 1509.
[20] A.I. Sabry, Phytochemical and biological study of certain Conyza species growing in Egypt, in: PHD. Thesis, Faculty of Pharmacy, Pharmacognosy Department, Beni-Suef, 2012.
[21] K. Khadayat, et al., Evaluation of the alpha-amylase inhibitory activity of Nepalese medicinal plants used in the treatment of diabetes mellitus, Clinical Phytoscience 6 (1) (2020) 1–8.
[22] H.M. Abdallah, et al., Phenolics from chrozophora oblongifolia aerial parts as inhibitors of α-glucosidases and advanced glycation end products: in-vitro assessment, molecular docking and dynamics studies, Biology 11 (5) (2022) 762.
[23] O. Herrera-Calderon, et al., Computational study of the phytochemical Constituents from uncaria tomentosa stem bark against SARS-CoV-2 omicron spike protein, J. Chem. 2022 (2022).
[24] S.B. Kedare, R. Singh, Genesis and development of DPPH method of antioxidant assay, J. Food Sci. Technol. 48 (2011) 412–422.
[25] S. El Zalabani, et al., Antihyperglycemic and antioxidant activities and chemical composition of Conyza dioscoridis (L.) Desf. DC. growing in Egypt, Aust. J. Basic Appl. Sci 6 (10) (2012) 257–265.
[26] H.A. Jung, et al., Prunin is a highly potent flavonoid from Prunus davidiana stems that inhibits protein tyrosine phosphatase 1B and stimulates glucose uptake in insulin-resistant HepG2 cells, Arch Pharm. Res. (Seoul) 40 (2017) 37–48.
[27] V. Shilpa, et al., Phytochemical properties, extraction, and pharmacological benefits of naringin: a review, Molecules 28 (15) (2023) 5623.
[28] G. Faccio, et al., Bacterial tyrosinases and their applications, Process Biochem. 47 (12) (2012) 1749–1760.
[29] Y. Yuan, et al., Tyrosinase inhibitors as potential antibacterial agents, Eur. J. Med. Chem. 187 (2020) 111892.